

Radio-frequency-mediated dipolar recoupling among half-integer quadrupolar spins

Marc Baldus,^{a)} David Rovnyak, and Robert G. Griffin

Francis Bitter Magnet Laboratory and Department of Chemistry, Massachusetts Institute of Technology, Cambridge, Massachusetts 02139

(Received 10 September 1999; accepted 17 December 1999)

It is demonstrated that through-space recoupling can be achieved in dipolar coupled quadrupolar spins in the presence of an appropriate radio-frequency field. Experimental and theoretical results for ^{23}Na – ^{23}Na pairs are presented that elucidate the experimental conditions leading to homonuclear dipolar transfer. The effect of adiabatic amplitude modulation on spin-3/2 systems is compared to spin-1/2 cases and applications of this approach in the context of high resolution multi-quantum magic angle spinning for dipolar filtering and correlation are discussed. © 2000 American Institute of Physics. [S0021-9606(00)01810-9]

I. INTRODUCTION

Homonuclear correlation spectroscopy¹ represents one of the key experiments in nuclear magnetic resonance (NMR) to elucidate molecular spin topologies and short-range interactions in liquid^{1,2} and solid-phase materials.^{1,3} In solid-state NMR, magic angle spinning⁴ (MAS) has become one of the premier techniques to establish high-resolution conditions. Subsequently, substantial progress has been made by a variety of techniques to retrieve through-space information in spin-1/2 systems under MAS where the dipolar interaction is usually suppressed. On the other hand, structural information in quadrupolar spin systems based on dipolar or scalar couplings has been scarce. Quadrupolar nuclei not only can be used as sensitive probes of local order and structuring in material science applications⁵ but are also regularly found in a large number of chemical and biological processes ranging from catalytic compounds to metallo- or membrane proteins.^{5,6} In general, homonuclear dipolar correlation spectroscopy can provide valuable structural information whenever multiple quadrupolar sites are expected in close spatial proximity.

Unfortunately, most spin-1/2 methods involving radio frequency (rf) irradiation (for recent comparative studies see, e.g., Refs. 7 and 8) are not readily applicable in quadrupolar spin systems because of unwanted interference effects with the dominating quadrupolar coupling. In cases where dynamic angle spinning^{5,9} (DAS) probes are available and relaxation times are favorable, dipolar transfer can be established by rapidly switching the spinning assembly away from the magic angle.¹⁰ Dipolar transfer is not suppressed for sample spinning away from the magic angle orientation and this approach has been successfully utilized in quadrupolar spin systems.¹¹ However, anisotropic interactions such as the quadrupolar coupling and chemical shielding interactions (CSA) also remain resulting in complicated powder line shapes that usually need to be described by computational

methods. For this reason, a correlation technique that enables dipolar transfer under MAS would be desirable.

In this contribution, we show that it is possible to achieve dipolar recoupling employing radio frequency fields under conventional MAS conditions. In the spin-1/2 case the dipolar interaction must be recovered without additional destructive interference from isotropic or anisotropic chemical shielding interactions. In quadrupolar spin systems two additional challenges need to be addressed.

(a) In contrast to the spin-1/2 case, where isotropic chemical shifts are the only remaining interaction under high-frequency MAS, quadrupolar MAS spectra are broadened by anisotropic second order interactions that usually lead to a powder distribution. In the context of dipolar recoupling, these second order couplings behave in a manner similar to that observed for a static $I = 1/2$ system. That is, they represent orientation-dependent chemical shift terms (CSA) that perturb the dipolar transfer in the laboratory frame and these terms must be suppressed by appropriate rf schemes.

(b) One of the design principles in spin-1/2 recoupling experiments relates to the fact that rf fields can usually be assumed to dominate the spin system Hamiltonian. As a consequence, spin locking and nutation of NMR coherences is not affected by the size of other system interactions. In contrast, the quadrupolar interaction remains the dominating interaction, even if modulated by MAS or if in the presence of strong rf fields. Thus care needs to be taken in designing an rf driven recoupling experiment that can be used in a regime where spin locking is achievable.

We will show in the following that both criteria can be fulfilled to a good extent by modifying a rotary resonance phenomenon first observed in spin-1/2 systems in the presence of dipolar^{12,13} and CSA¹⁴ interactions. These effects have been utilized to study local spin geometries under MAS,^{15,16} in the context of adiabatic two-dimensional correlation spectroscopy in spin-1/2 systems¹⁷ and for dipolar filtering.¹⁸

For the theoretical description we will use the concept of fictitious spin-1/2 operators^{19–21} and derive an effective di-

^{a)}Current address: Gorlaeus Laboratories, Leiden University, 2333 CC Leiden, The Netherlands.

polar recoupling Hamiltonian in close analogy to the spin-1/2 case. The transfer characteristics also allow for the discrimination between local spatial proximity and exchange phenomena, e.g., relevant in a number of biological systems. Finally, we discuss experimental variations that permit integration of dipolar recoupling with MQMAS.²²

II. THEORY

Our goal is to study rotary resonance in a dipolar coupled quadrupolar two-spin system. Since the effects of MAS and concomitant application of rf fields are more complicated than in spin-1/2 applications, we will first present a brief theoretical analysis of the spin-locking behavior of an isolated spin-3/2 nucleus.

A. Isolated spin-3/2 nucleus

In the high field approximation and under rapid MAS at Θ_M , the quadrupolar Hamiltonian is given to second order by^{5,23-25}

$$H_Q = H_Q^{(1)}(t) + H_Q^{(2)}(t) \quad (1)$$

with

$$H_Q^{(1)}(t) = A_{20}(t)T_{20}, \quad (2)$$

$$H_Q^{(2)}(t) = \frac{1}{\omega_0} \sum_{m=\pm 1, \pm 2} \frac{1}{m} A_{2m}(t)A_{2-m}(t)[T_{2m}, T_{2-m}],$$

and

$$A_{2m}(t) = \sum_{n=\pm 1, \pm 2} A_{2n}(\alpha, \beta, \gamma) d_{nm}(\Theta_M) \exp[in\omega_R t]. \quad (3)$$

The quadrupolar tensor elements $A_{2n}(\alpha, \beta, \gamma)$ in the rotor fixed axis system depend on the relative orientation [described by the Euler angles (α, β, γ)] of the PAS to the rotor fixed axis system. The definition of the spatial $A_{2n}(\alpha, \beta, \gamma)$ and spin tensor components T_{2m} can be found in Ref. 25. Even under rapid sample spinning, the second order contribution is not suppressed and a time independent, $H_{Q,iso}^{(2)}$, contribution remains

$$H_{Q,iso}^{(2)} = \omega_Q^{21}(\alpha, \beta)[T_{21}, T_{2-1}] + \omega_Q^{22}(\alpha, \beta)[T_{22}, T_{2-2}] \quad (4)$$

with $\omega_Q^{2k}(\alpha, \beta) = (1/\omega_0)f_k(\alpha, \beta)$ ($k=1,2$). An explicit definition of the anisotropic factors $f_k(\alpha, \beta)$ is given in Appendix A. Equation (4) leads to the well-known powder distribution that scales as ω_0^{-1} .

In the following, we will concentrate on the spin $I=3/2$ case and study experimental conditions that promote dipolar recoupling between quadrupolar spins. For this analysis it is convenient to rewrite Eq. (4) in terms of fictitious spin-1/2 operators:¹⁹⁻²¹

$$H_{Q,iso}^{(2)} = \Omega_Q^{2-3}(\alpha, \beta)I_z^{2-3} + \Omega_Q^{1-4}(\alpha, \beta)I_z^{1-4}. \quad (5)$$

Under high frequency MAS, an isolated quadrupolar spin in the presence of isotropic chemical shifts and rf fields may be then approximated by

$$H = H_{rf} + H_\Omega + H_Q^{(1)}(t) \quad (6)$$

with

$$\begin{aligned} H_{rf} &= \omega_{rf}(2I_x^{2-3} + \sqrt{3}(I_x^{1-2} + I_x^{3-4})), \\ H_\Omega &= (\Omega_{CS}^{2-3} + \Omega_Q^{2-3}(\alpha, \beta))I_z^{2-3} \\ &\quad + ((\Omega_{CS}^{1-4} + \Omega_Q^{1-4}(\alpha, \beta)))I_z^{1-4}, \\ H_Q^{(1)}(t) &= A_{20}(t)/\sqrt{6}[I_z^{1-2} - I_z^{3-4}]. \end{aligned} \quad (7)$$

Valuable insight into the spin dynamics of a Hamiltonian such as Eq. (7) was outlined by Vega^{26,27} by monitoring the adiabatic evolution of eigenstates and eigenvalues. In these studies, it was observed that the central transition coherence can be spin locked (i.e., $[I_x^{2-3}, H]=0$) whenever $\alpha = \omega_{rf}^2/\omega_Q\omega_R \ll 1$ using the effective quadrupolar coupling $\omega_Q = (3e^2qQ)/(2I(2I-1)\hbar)$. According to this result, small rf fields and large spinning frequencies promote efficient spin locking. On the other hand, inspection of Eq. (7) provides a lower boundary for the rf field that must be applied to suppress time-independent chemical shift terms (given by H_Ω) in the 2-3 subspace:

$$Z\omega_{rf} > \Omega_{CS}^{2-3} + \Omega_Q^{2-3}(\alpha, \beta). \quad (8)$$

In a tilted frame in which the central transition coherence is diagonal, these chemical shift terms are nonsecular and can only be neglected if the rf field is sufficiently large to compensate for isotropic chemical shift (CS). Equation (8) also agrees with a recent study using Floquet theory.²⁸

To further examine the combined influence of rf irradiation and the MAS modulated quadrupolar coupling in Eq. (6), we transform to an interaction representation using $U = \exp[\int_0^t H_Q^{(1)}(t')dt']$. Using the commutation relations among multiquantum (MQ) coherences in the fictitious spin-1/2 space (see Appendix B), Eq. (6) reduces in this frame to

$$\tilde{H} = \tilde{H}_\Omega + \tilde{H}_{rf} \quad (9)$$

with $\tilde{H}_\Omega = H_\Omega$,

$$\begin{aligned} \tilde{H}_{rf} &= \omega_{rf}(2I_x^{2-3} + \sqrt{3}(\cos(\zeta(t))(I_x^{1-2} + I_x^{3-4}) \\ &\quad + \sin(\zeta(t))(I_y^{1-2} - I_y^{3-4})), \end{aligned} \quad (10)$$

and $\zeta(t) = 1/(\sqrt{6})\int_0^t A_{20}(t')dt'$. The observable of interest, I_x^{2-3} , is obtained by solving the Liouville-von Neuman equation:

$$\langle D(t) \rangle = \text{Tr}_1(\sigma(t)D) \quad (11)$$

with $\sigma(t) = U(t)\sigma(0)U^\dagger(t)$, $D = \sigma(0) = I_x^{2-3}$, and

$$U(t) = T \exp\left[-i \int_0^t \tilde{H}_{rf}(s)ds\right] \quad (12)$$

with the Dyson time-ordering operator T and the Hamiltonian of Eq. (10). Obviously, the first term in Eq. (10) will keep central transition coherence spin locked, but the explicit time dependence of the remaining terms complicates a further analytical solution of Eq. (11). As shown in Appendix C, we can qualitatively predict the time evolution by using the commutation relations of fictitious spin-1/2 operators. In agreement with numerical simulations shown in Ref. 29, these terms generate triple-quantum coherence in the context of strong (RIACT)³⁰ or weak to medium-size rf fields that match a multiple of the MAS spinning frequency.³¹ Spin

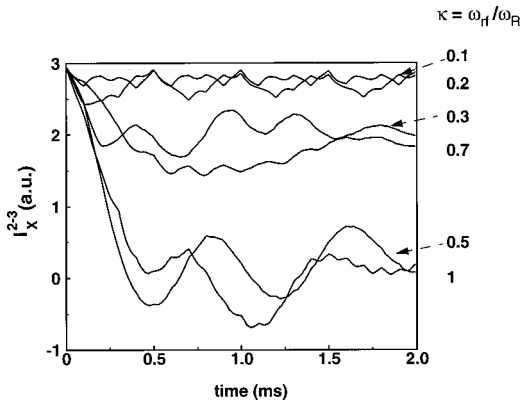


FIG. 1. Time evolution of central transition coherence as a function of applied rf field strength. Quadrupolar coupling and MAS spinning frequency were kept constant at 3 MHz and 10 kHz, respectively. All numerical simulations using Eq. (1) and the rf and chemical shift definitions of Eq. (7) were performed in the programming environment GAMMA. Perfect spin locking is described by the gray line. As expected, the spin-lock behavior generally decreases for increasing rf fields with minima at $\kappa = n/2$ ($n = 1, 2, \dots$). For values between (0.1–0.3) the time evolution can, to a good extent, be described by a spin-locked central transition coherence that is only weakly modulated by the time-dependent terms. These results are in qualitative agreement with additional simulations using different quadrupolar couplings and spinning frequencies.

locking relates to an experimental regime where the second and third term in Eq. (10) can be minimized. To give a more quantitative understanding of the spin-lock regime as a function of rf field strength, MAS spinning frequency and quadrupolar coupling, we performed numerical simulations using Eq. (1) and the rf and chemical shift definitions of Eq. (7) in the programming environment GAMMA.³² For all simulations discussed in the following the time dependence of the system Hamiltonian was described by the Floquet formalism³³ implemented in GAMMA³⁴ or using a piecewise constant approach.

In Fig. 1 the time evolution of the central transition coherence given by Eq. (11) is monitored as a function of the ratio of rf field and MAS frequency:

$$\kappa = \frac{\omega_{\text{rf}}}{\omega_R}. \quad (13)$$

Quadrupolar coupling and MAS spinning frequency were constant at 3 MHz and 10 kHz, respectively. As expected, the spin lock efficiency generally decreases for increasing rf fields with minima at $\kappa = n/2$ ($n = 1, 2, \dots$). These effects have previously been observed,^{31,35} and in the following we will assume that these settings are avoided. On the other hand, Fig. 1 indicates that for values of κ between (0.1–0.3) the time evolution can effectively be described by a spin-locked central transition coherence that is only weakly modulated by the time-dependent terms in Eq. (11). Additional calculations varying the quadrupolar parameters and the MAS frequency are in good agreement with these observations provided that Eq. (8) is not seriously violated.

B. Dipolar coupled $S=3/2$ system

In the following we assume that the rf fields and MAS spinning frequencies meet the criterion of spin locking [i.e.,

κ between (0.1–0.3) and Eq. (8) is fulfilled]. The effective rf field Hamiltonian then contains the central transition coherence operator. The combined effect of quadrupolar and rf field interactions in a dipolar coupled two-spin (IS -spin-3/2) system can thus be summarized by

$$H = 2\omega_{\text{rf}}(I_x^{2-3} + S_x^{2-3}) + H_D + H_{\text{CS}}, \quad (14)$$

with

$$H_D = D(t)(3I_z S_z - \vec{I}\vec{S}), \quad (15)$$

$$H_{\text{CS}} = (\Omega_{I,\text{CS}}^{2-3} + \Omega_{I,Q}^{2-3}(\alpha, \beta))I_z^{2-3} + (\Omega_{S,\text{CS}}^{2-3} + \Omega_{S,Q}^{2-3}(\alpha, \beta))S_z^{2-3}.$$

Note that in contrast to the spin-1/2 case, orientation-dependent chemical shifts terms $\Omega_{k,\text{CS},Q}(\alpha, \beta) = \Omega_{k,\text{CS}}^{2-3} + \Omega_{k,Q}^{2-3}(\alpha, \beta)$ ($K = I, S$) remain. In Eq. (15), we have neglected the isotropic chemical shift term in the 1–4 subspace since to zeroth order it will not be affected by rf irradiation in Eq. (14). $D(t)$ represents the MAS modulated dipolar coupling and is given by

$$D_{\pm 1} = \frac{D'}{2\sqrt{2}} \sin(2\beta_d) e^{\pm i\gamma_d},$$

$$D_{\pm 2} = \frac{D'}{4} \sin^2(\beta_d) e^{\pm 2i\gamma_d}, \quad (16)$$

$$D' = \frac{\mu_0 \gamma_I^2 h}{4\pi r^3},$$

β_d and γ_d are the polar angles that describe the direction of the internuclear dipolar vector \vec{r} in a rotor-fixed coordinate system with its z axis along the sample rotation axis. γ_I represent the gyromagnetic ratio of spin I . For spin-3/2, the dipolar Hamiltonian of Eq. (15) can be rewritten using the definition of the angular momentum operators:

$$\Lambda_x = \sqrt{3}(\Lambda_x^{1-2} + \Lambda_x^{3-4}) + 2\Lambda_x^{2-3},$$

$$\Lambda_y = \sqrt{3}(\Lambda_y^{1-2} + \Lambda_y^{3-4}) + 2\Lambda_y^{2-3}, \quad (17)$$

$$\Lambda_z = 3\Lambda_z^{1-4} + \Lambda_z^{2-3}$$

with $\Lambda = I, S$. Combining Eqs. (17) and (15), terms that are bilinear in the 2–3 subspace are readily isolated:

$$H_{D,\text{eff}}^{2-3,2-3} = 2D(t)(I_z^{2-3} S_z^{2-3} - 2I_x^{2-3} S_x^{2-3} - 2I_y^{2-3} S_y^{2-3}). \quad (18)$$

Since we are interested in double-quantum (DQ) recoupling conditions in the 2–3 subspace, all additional terms that result from combining Eqs. (17) and (15) can be neglected. DQ recoupling between spin I and S can now be studied by using a tilted frame with $\omega_{k,\text{eff}}(\alpha, \beta) = \sqrt{\Omega_{k,\text{CS},Q}(\alpha, \beta)^2 + (2\omega_{\text{rf}})^2}$ along the new Z axis (see Fig. 2), i.e.,

$$\Lambda_Z = \cos \theta_k \Lambda_z + \sin \theta_k \Lambda_x,$$

$$\Lambda_X = (-\sin \theta_k) \Lambda_z + \cos \theta_k \Lambda_x, \quad (19)$$

$$\Lambda_Y = \Lambda_y,$$

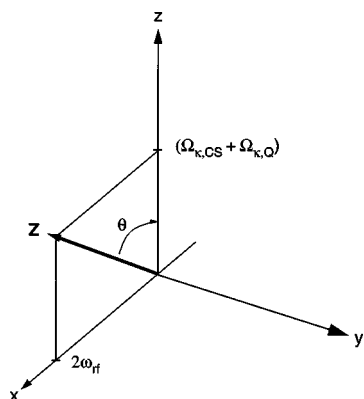


FIG. 2. Graphical representation of the tilted frame used in the 2–3 subspace to describe dipolar recoupling. The tilt angle θ is defined in the text.

with $\theta_k = \arctan(2\omega_{\text{rf}}/\Omega_{k,CS,Q}(\alpha, \beta))$ and $\Lambda = I^{2-3}, S^{2-3}$. A subsequent transformation into an interaction frame defined by

$$U_{\text{eff}} = \exp[-i\omega_{I,\text{eff}}(\alpha, \beta)I_z^{2-3}] \exp[-i\omega_{S,\text{eff}}(\alpha, \beta)S_z^{2-3}] \quad (20)$$

allows to investigate interference effects between the mechanical sample rotation and the rf irradiation. In a dipolar coupled spin-1/2 system an analogous procedure has been shown to result in double-, single-, and zero-quantum transfer conditions.³⁶ In close analogy, double-quantum dipolar recoupling will be established by the effective Hamiltonian ($\Lambda = I^{2-3}, S^{2-3}$)

$$H = Q(\theta_I, \theta_S) d_n (I_+^{2-3} S_+^{2-3} + I_-^{2-3} S_-^{2-3}) \quad (21)$$

with $Q(\theta_I, \theta_S) = [1 - 2 \cos(\theta_I) \cos(\theta_S) + 2 \sin(\theta_I) \sin(\theta_S)]$ and $\Lambda_{\pm} = \Lambda_x \pm i\Lambda_y$. The effective dipolar coupling d_n results from Eq. (16) using $D_n = d_n \exp[\pm in\gamma_d]$ and the general (dipolar double-quantum) recoupling condition is given by

$$\omega_{I,\text{eff}}(\alpha, \beta) + \omega_{S,\text{eff}}(\alpha, \beta) = n\omega_R. \quad (22)$$

Note that this result is analogous to the spin-1/2 treatment except for the effective nutation frequency that is a factor 2 larger than in the spin-1/2 case and the anisotropic chemical shift dispersion due to the occurrence of the quadrupolar couplings. Equations (21) and (22) result from transforming the bilinear terms of Eq. (18). In addition, single- and zero-quantum recoupling conditions can be established that connect both 2–3 subspaces or, unlike to the spin-1/2 situation, recouple the 2–3 and 1–4 subspaces of the I and S spins, respectively. These recoupling conditions are given by

$$\omega_{k,\text{eff}}(\alpha, \beta) = n\omega_R, \quad k = I, S, \quad (23a)$$

$$\omega_{I,\text{eff}}(\alpha, \beta) - \omega_{S,\text{eff}}(\alpha, \beta) = n\omega_R, \quad (23b)$$

and generally require larger rf fields, i.e., larger values of κ . In the particular case of single quantum recoupling, 2–3 and 1–4 (I, S) subspaces are recoupled simultaneously—in addition to the (spin-1/2 analogous) $I(2-3), S(2-3)$ condition. As in the spin-1/2 case, significant signal loss results. To avoid these effects, we will in the following assume rf fields and MAS frequencies which approximately satisfy Eq. (22).

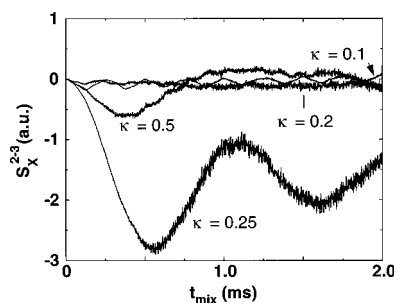


FIG. 3. Numerical simulation of dipolar recoupling in a dipolar coupled quadrupolar two-spin system. At time $t=0$, the system is prepared with central transition coherence on the first (i.e., I) spin and the polarization transfer on spin S is monitored for different rf fields. The MAS spinning frequency is kept constant. Only for the recoupling conditions discussed in the text, substantial polarization transfer is observed in agreement with the theoretical predictions.

These theoretical predictions are also supported by numerical simulations in GAMMA for an isolated (I, S) spin-3/2 spin system and are shown in Fig. 3. Quadrupolar couplings of 1.2 MHz and 2.4 MHz were assumed for I and S spin, respectively. A homonuclear dipolar coupling of 2 kHz was assumed. The spin system is initially prepared with 2–3 coherence on spin I and the signal according to Eq. (11) is monitored with $D = S_x^{2-3}$. For the numerical calculations, rf, quadrupolar and dipolar interactions were included as given in Eqs. (1), (7), and (15), respectively. To simplify the analysis, a chemical shift offset was chosen that matches the isotropic quadrupolar second-order contribution. In this case, the effective field is identical to the rf field and recoupling should occur for $\kappa=0.25$ and $\kappa=0.5$. Indeed, negative coherence transfer characteristic for a double-quantum Hamiltonian³⁷ is observed with higher efficiency at the $n=1$ (i.e., $\kappa=0.25$) condition. As stated earlier this condition is preferable in order to avoid unwanted SQ conditions that—as indicated in Fig. 3 for $\kappa=0.5$ —significantly diminish the transfer efficiency. In addition, Eq. (21) indicates that the dipolar coupling element is larger [see Eq. (16)] for the $n=1$ condition. Further, these results are in agreement with calculations of a complete two-dimensional recoupling experiment (discussed in the following) and indicate the occurrence of negative cross-peaks regions which are also observed in spin-1/2 applications.³⁷

Due to the presence of orientation-dependent isotropic shifts, the recoupling condition of Eq. (22) cannot be fulfilled for all spins simultaneously. However, using an amplitude modulation $\omega_{\text{rf}} \rightarrow \omega_{\text{rf}}(t_{\text{mix}})$ establishes the recoupling condition for a larger number of crystallites during the mixing time of a 2D correlation experiment. This technique has previously been demonstrated in homonuclear spin-1/2 applications.^{17,18} The range of rf fields used in the experiment and presented in the following were restricted to the regime $\kappa(t) = \frac{1}{4} \pm \frac{1}{4}, t \in [0, T]$ using tangential amplitude shapes.³⁸

III. EXPERIMENTS

The method discussed above was experimentally tested on anhydrous Na_2HPO_4 that has been shown to contain three

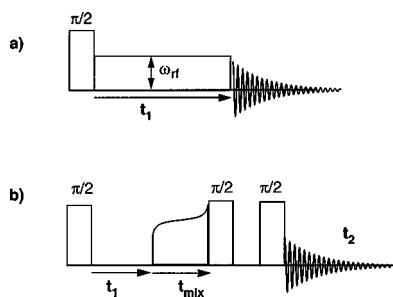


FIG. 4. (a) Experimental protocol to observe central transition coherence as a function of spin-lock time t or rf field strength ω_{rf} . (b) Two-dimensional dipolar correlation experiments to observe recoupling among different quadrupolar sites. All $\pi/2$ are adjusted to give central transition coherence only. After the conventional evolution time t_1 , dipolar recoupling occurs during the mixing time t_{mix} in which the rf field close to the $\kappa=0.25$ is modulated by a tangential shape. Subsequently, a z filter is employed to remove any unwanted coherences.

distinct Na sites in the unit cell.²⁵ Quadrupolar and chemical shift parameters have been determined previously and indicate that MAS spinning frequencies of 8 kHz or higher are sufficient to suppress MAS sidebands at fields at or above 500 MHz [see also Fig. 5(a)].

The rf fields were determined approximately using NaBr. To identify rf amplitudes that fulfil the conditions outlined in Eq. (22) more precisely, a spin-lock experiment as outlined in Fig. 4(a) was performed on Na_2HPO_4 and is shown in Fig. 5(b). Here, the central transition coherence is monitored after a spin-lock time of 1 ms as a function of the size of the applied rf field strength. As discussed in the preceding section and shown in Fig. 5(b), we observe characteristic resonance minima at $\kappa=n/2$, $n=1,2$ for a MAS frequency of 8.3 kHz. In addition, a small signal minimum around $\kappa=0.25$ is observed, indicative of a DQ recoupling

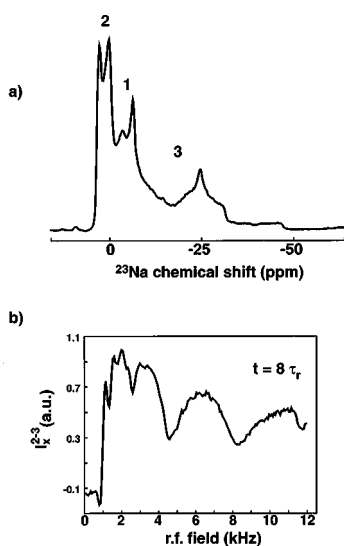


FIG. 5. (a) ^{23}Na MAS spectrum of anhydrous Na_2HPO_4 at 10 kHz spinning frequency and 11.7 T magnetic field strength. Chemical shift values are referenced to 0.1 M NaCl. Numbering of the three Na sites corresponds to the analysis performed in Ref. 25. (b) Central transition coherence in Na_2HPO_4 as a function of rf field strength for the indicated spin-locking time and a MAS frequency of 8.3 kHz. A one-dimensional slice along the Na(1) (see also Ref. 25) is shown.

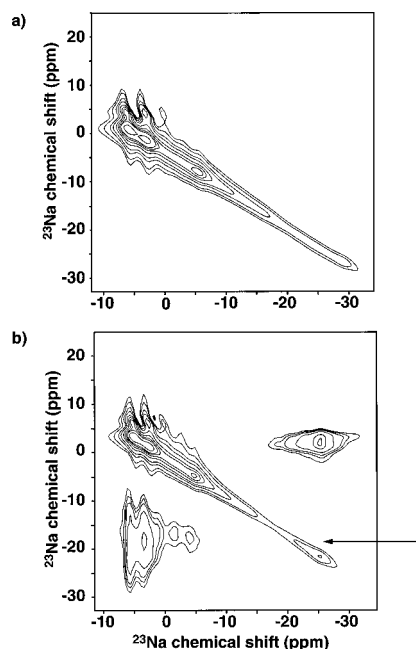


FIG. 6. Two-dimensional correlation patterns on anhydrous Na_2HPO_4 for mixing times of 0.5 (a) and 6 ms (b), respectively. Positive contour levels (along the diagonal) are shown in linear increments from 5–20%. All contour levels in the cross peak region visible in (b) are negative.

effect. In general, dipolar induced DQ coherence recoupling will lead to signal decrease of the central transition coherence $I_x^{2-3} + S_x^{2-3}$. The characteristic minima observed in Fig. 5(b) are observable across the entire MAS line shape shown in Fig. 5(a).

Next, we recorded a 2D recoupling experiment following the experimental protocol outlined in Fig. 4(b). Phase sensitive detection was accomplished using the method of Ruben *et al.*³⁹ and all $\pi/2$ pulses used rf fields in the order of 5–10 kHz to ensure efficient excitation of only the central transition coherence. In addition, MAS experiments using proton decoupling during data acquisition and 2D proton-driven spin-diffusion experiments (see, e.g., Refs. 40 and 41) were performed. It was found that the influence of hetero- or homonuclear dipolar couplings to surrounding protons can be neglected. Further experimental details can be found in the caption.

In Fig. 6 the experimental results for two different mixing times are displayed. As expected, no cross peak intensities are observed for vanishing or very short mixing times [Fig. 6(a)]. The carrier frequency was set at approximately the value to fulfil the spin-lock criterion of Eq. (22) for all spins at a small carrier offset. In Fig. 6(b) the contour pattern after 6 ms mixing is illustrated and significant negative intensities are observable across the entire map. Unlike to *static* correlation experiments using proton or rf driven transfer techniques (see, e.g., Refs. 40 and 41), the cross-peak regions feature negative intensities which, close to the diagonal, lead to a partial cancellation of signal intensity. For this reason, only regions with the highest negative cross peak intensities are displayed.

The data obtained in Fig. 6(b) clearly indicate dipolar correlations among different parts of the MAS spectrum in

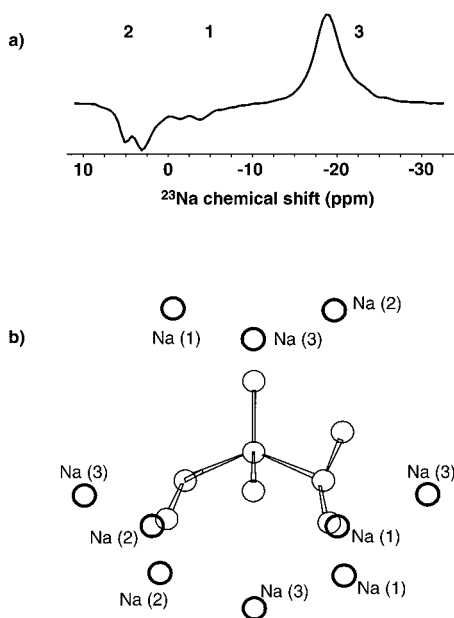


FIG. 7. (a) One-dimensional slice along the position indicated by the arrow in Fig. 6(b) that reveals negative signal intensities in the cross peak region. Numbering indicates the approximate resonance regime where the three distinct Na sites (as defined in Ref. 25) are found. (b) Plot of the local environment of the HPO_4^{2-} anions [according to Baldus *et al.* (Ref. 25)] that reveals the local arrangement of the Na sites.

Na_2HPO_4 . In this particular case, the three Na sites contributing to the overall signal can mostly be confined to three different regions of the spectrum. Comparing the results and the renewed x-ray structure the most significant cross peak intensities are found for the (Na1, Na2) and (Na2, Na3) pairs (numbering as in Ref. 25) in accordance with the closest distances in the unit cell [shown in Fig. 7(b)]. However, the broadband amplitude modulation establishes dipolar transfer among all three spins during the mixing period and therefore care must be taken to relate the observed cross peak intensities to intermolecular distances. This broadband recoupling behavior is visible from the 1D slice shown in Fig. 7(a) that indicates negative cross peak intensities across the entire line shape. These effects could be taken into account by performing a numerical simulation of the recoupling pattern similar to techniques used for the analysis of static tensor correlations.^{40–42}

Additional experimental results indicate that varying the carrier frequency by several kHz can be used to enhance or suppress the dipolar transfer in particular subsections of the spectrum. This is due largely to the fact that the isotropic chemical shift suppression is accomplished by an amplitude sweep, which, for the experimental conditions of Figs. 6 and 7 are of the order of several kHz. Since off-resonance rf irradiation generally decreases the spin-locking efficiency [Eq. (8)], an rf carrier close to the isotropic chemical shifts of the spin system under study is preferable.

The presented techniques are most efficient in systems where the chemical shift dispersion among different sites with significant quadrupolar couplings is small. Since the efficiency of the spin locking only interferes with sites of medium to large (i.e., larger than 1–2 MHz) quadrupolar

couplings, the carrier frequency should be set close to the on-resonance case for these sites. Finally, it is also possible to combine the approach described here with the MQMAS method²² to achieve a high-resolution dimension. Since recoupling occurs in the 2–3 subspace, the technique can be inserted after MQ reconversion and prior to acquisition. This approach introduces (if applied as shown in Fig. 4) an additional evolution dimension that will increase the overall experiment time. Alternatively, the conventional MQMAS experiment can be modified to achieve a high-resolution dimension in a 2D correlation experiment. As demonstrated by Wimperis *et al.*⁴³ amplitude- or phase-modulated “split- t_1 ” MQMAS experiments can be used to fully refocus the second-order broadening during the evolution period of an MQMAS experiment. The homonuclear recoupling technique discussed here could be inserted after MQ reconversion and would yield a 2D dipolar correlation spectrum with a high resolution dimension along t_1 .

IV. CONCLUSIONS

Homonuclear polarization transfer represents one of the key elements for structure elucidation in spin-1/2 applications. A number of techniques are available for assignments, distance and torsion angle determination.^{42,44}

In this contribution we have demonstrated that dipolar recoupling can also be achieved in quadrupolar spin systems. As long as an rf field strength is used that allows for spin locking in the order of ms, dipolar correlations in ^{23}Na of 3–6 Å can be probed. The technique depicted here is efficient in systems where the isotropic chemical shift dispersion is small (such as Na^{23}) and where the width of the second-order quadrupolar broadening does not exceed the range of MAS frequencies. The latter aspect can generally be improved by using higher magnetic fields. Even at the highest obtainable spinning frequencies, the experiment is very forgiving with respect to the size of the applied rf field strength, and thus can be employed using readily available hardware. The experiment should be designed to minimize signal losses due to off-resonance nutation and amplitude modulations where $\kappa \in [0.1, 0.3]$ are preferred.

Since the present approach involves double-quantum transfer in the rotating frame, the method promises to be useful in the context of discriminating between chemical exchange processes and spatial proximity. Similar approaches are routinely used in liquid state NMR.⁴⁵ It is, e.g., well known^{46,47} that exchange processes between free and protein bound molecules occur in solid-phase membrane proteins. The results described here could be used to study correlations as a function of temperature and concentration in cationic solvents.

The methods are also extendable to multidimensional correlation studies involving spin-1/2 nuclei. Double quantum coherence created during the homonuclear transfer step could also be detected using pulsed field gradients.⁴⁸

Finally, it is also possible to combine the approach with the MQMAS method to achieve a high-resolution dimension during a multidimensional correlation experiment. Different approaches have been discussed and are currently under experimental study.

ACKNOWLEDGMENTS

We thank Dr. C. M. Rienstra and Dr. J. D. Gross for fabrication of the MAS probes used in this research. M. B. gratefully acknowledges financial support by the German Research Society (DFG). This work was supported by Grant Nos. GM-23403 and RR-00995.

APPENDIX A

Using the explicit definition of the MAS modulated spatial tensor elements $A_{2m}(t)$, Eq. (2) can be rewritten as

$$H_Q^{(2)}(t) = \frac{1}{\omega_0} \sum_{\substack{m=\pm 1, \pm 2 \\ k=\pm 1, \pm 2 \\ l=\pm 1, \pm 2}} \frac{1}{m} A_{2k}(\alpha, \beta, \gamma) d_{km}(\Theta_M) \\ \times A_{2l}(\alpha, \beta, \gamma) d_{l-m}(\Theta_M) [T_{2m}, T_{2-m}] \\ \times \exp[i(k+l)\omega_R t]. \quad (\text{A1})$$

Time-independent contributions result if $k = -l$ and can be described by Eq. (4) using the following definitions:

$$f_1(\alpha, \beta) = \sum_{k=\pm 1, \pm 2} A_{2k}(\alpha, \beta, \gamma) A_{2-k}(\alpha, \beta, \gamma) \\ \times (d_{k1}(\Theta_M) d_{-k-1}(\Theta_M) \\ + d_{k-1}(\Theta_M) d_{-k1}(\Theta_M)), \quad (\text{A2}) \\ f_2(\alpha, \beta) = \sum_{k=\pm 1, \pm 2} \frac{1}{2} A_{2k}(\alpha, \beta, \gamma) A_{2-k}(\alpha, \beta, \gamma) \\ \times (d_{k2}(\Theta_M) d_{-k-2}(\Theta_M) \\ + d_{k(-2)}(\Theta_M) d_{-k2}(\Theta_M)).$$

The explicit definitions of the reduced Wigner elements $d_{kl}(\theta)$ can be found in Ref. 23.

APPENDIX B

The propagator U leading to the transformation $\tilde{H} = UHU^\dagger$ can be defined by

$$U = \exp[i\zeta(t)(I_z^{1-2} - I_z^{3-4})] \quad (\text{B1})$$

with $\zeta(t) = 1/\sqrt{6} \int_0^t A_{20}(s) ds$ and H as given in Eq. (6). For two fictitious spin-1/2 operators P and Q that fulfil $[P, Q] = i\kappa R$ the transformation rule

$$\exp[-i\theta P] Q \exp[i\theta P] = Q \cos \kappa\theta + R \sin \kappa\theta \quad (\text{B2})$$

can be derived. Using $P = (I_z^{1-2} - I_z^{3-4})$ and the general commutations relations as given in Refs. 19 and 20 we find

$$[(I_z^{1-2} - I_z^{3-4}), I_x^{2-3}] = [I_z^{1-2}, I_x^{2-3}] - [I_z^{3-4}, I_x^{2-3}] = 0, \\ [(I_z^{1-2} - I_z^{3-4}), (I_x^{1-2} + I_x^{3-4})] = i(I_y^{1-2} - I_y^{3-4}), \\ [(I_z^{1-2} - I_z^{3-4}), I_z^{2-3}] = 0, \quad (\text{B3}) \\ [(I_z^{1-2} - I_z^{3-4}), I_z^{1-4}] = 0.$$

Using Eqs. (B2) and (B3), Eq. (10) is obtained.

APPENDIX C

Using

$$e^{iA} B e^{-iA} = B + i[A, B] - \frac{1}{2}[A, [A, B]] \\ + \frac{i}{3}[A, [A, [A, B]]] + \dots \quad (\text{C1})$$

we can qualitatively predict the time evolution of the central transition coherence I_x^{2-3} under the effective Hamiltonian of Eq. (10). Obviously, the first term in Eq. (10) represents the spin-locking part of the Hamiltonian and we can concentrate on the cos/sin modulated components of Eq. (10). For the cos-modulated part we can identify

$$A = I_x^{1-2} + I_x^{3-4}, \\ B = I_x^{2-3}, \quad (\text{C2})$$

and use the commutations relations given in Refs. 19 and 20. We obtain

$$[A, B] = [I_x^{1-2} + I_x^{3-4}, I_x^{2-3}] = [I_x^{1-2}, I_x^{2-3}] + [I_x^{3-4}, I_x^{2-3}] \\ = \frac{i}{2}(I_y^{1-3} - I_y^{2-4}) \quad (\text{C3})$$

and, subsequently

$$[A, [A, B]] = \left[I_x^{1-2} + I_x^{3-4}, \frac{i}{2}(I_y^{1-3} - I_y^{2-4}) \right] \\ = \frac{1}{2}(I_z^2 - I_z^{1-4}). \quad (\text{C4})$$

For the sin-modulated part of the effective rf field we obtain

$$[A, B] = [I_y^{1-2} - I_y^{3-4}, I_x^{2-3}] = [I_y^{1-2}, I_x^{2-3}] - [I_y^{3-4}, I_x^{2-3}] \\ = \frac{-i}{2}(I_x^{1-3} + I_x^{2-4}) \quad (\text{C5})$$

and, subsequently

$$[A, [A, B]] = \left[I_y^{1-2} - I_y^{3-4}, -\frac{i}{2}(I_x^{1-3} + I_x^{2-4}) \right] \\ = \frac{1}{2}(I_z^{2-3} - I_z^{1-4}). \quad (\text{C6})$$

From Eqs. (C4) and (C6), we find that the effective rf Hamiltonian of Eq. (10) connects 2–3 and 1–4 coherences in an MAS modulated manner. As a result, RIACT MQ excitation and reconversion occurs for strong rf fields or rotary resonance recoupling of MQ coherences can be established if the rf field matches the MAS frequency.³¹

¹R. R. Ernst, G. Bodenhausen, and A. Wokaun, *Principles of Nuclear Magnetic Resonance in One and Two Dimensions* (Clarendon, Oxford, 1987).

²K. Wüthrich, *NMR of Proteins and Nucleic Acids* (Wiley-Interscience, New York, 1986).

³M. Mehring, *Principles of High Resolution NMR in Solids* (Springer-Verlag, Berlin, 1983).

⁴E. R. Andrew, A. Bradbury, and R. G. Eades, *Nature (London)* **182**, 1659 (1958); I. J. Lowe, *Phys. Rev. Lett.* **2**, 285 (1959); E. R. Andrew, A. Bradbury, and R. G. Eades, *Nature (London)* **183**, 1802 (1959).

⁵See e.g., C. P. Slichter, *Principles of Magnetic Resonance* (Springer-Verlag, Berlin, 1978); D. Freude and J. Haase, *NMR Basic Principles and Progress* (Springer-Verlag, Berlin, 1993), Vol. 29; B. F. Chmelka and J. W. Zwanziger, *Quadrupole Effects in Solid-State Magnetic Resonance*,

- Vol. 33 of NMR Basic principles and progress (Springer-Verlag, Berlin, 1994).
- ⁶S. J. Lippard, *Progress in Inorganic Chemistry: Bioinorganic Chemistry* (Wiley, New York, 1990), Vol. 38.
- ⁷A. E. Bennett, R. G. Griffin, and S. Vega, *Solid-State NMR IV* (Springer-Verlag, Berlin, 1994), Vol. 33, p. 1.
- ⁸M. Baldus, D. G. Geurts, and B. H. Meier, *Solid State Nucl. Magn. Reson.* **11**, 157 (1998).
- ⁹K. T. Mueller, B. Q. Sun, G. C. Chingas, J. W. Zwanziger, T. Terao, and A. Pines, *J. Magn. Reson.* **127**, 470 (1990).
- ¹⁰M. Tomaselli, B. H. Meier, M. Baldus, J. Eisenegger, and R. R. Ernst, *Chem. Phys. Lett.* **225**, 131 (1994).
- ¹¹P. Hartmann, C. Jaeger, and J. W. Zwanziger, *Solid State Nucl. Magn. Reson.* **13**, 245 (1999).
- ¹²T. G. Oas, R. G. Griffin, and M. H. Levitt, *J. Chem. Phys.* **89**, 692 (1988).
- ¹³N. C. Nielsen, H. Bildsoe, H. Jakobsen, and M. H. Levitt, *J. Chem. Phys.* **101**, 1805 (1994).
- ¹⁴Z. H. Gan and D. M. Grant, *Mol. Phys.* **67**, 1419 (1989).
- ¹⁵Z. Gan and R. R. Ernst, *J. Chem. Phys.* **108**, 9444 (1998).
- ¹⁶M. Bak and N. C. Nielsen, *J. Chem. Phys.* **106**, 7587 (1997).
- ¹⁷M. Baldus, J. van Os, and B. H. Meier, poster P247, 38th ENC, Orlando, Florida, 1997.
- ¹⁸R. Verel, M. Baldus, M. Ernst, and B. H. Meier, *Chem. Phys. Lett.* **287**, 421 (1998).
- ¹⁹A. Wokaun and R. R. Ernst, *J. Chem. Phys.* **67**, 1752 (1977).
- ²⁰S. Vega, *J. Chem. Phys.* **68**, 5518 (1978).
- ²¹S. Vega and Y. Naor, *J. Chem. Phys.* **75**, 75 (1981).
- ²²(a) L. Frydman and J. S. Harwood, *J. Am. Chem. Soc.* **117**, 5367 (1995); (b) A. Medek, J. S. Harwood, and L. Frydman, *ibid.* **117**, 12779 (1995).
- ²³B. Q. Sun, Ph.D. thesis, University of California, Berkeley, 1991.
- ²⁴J. Skibsted, N. C. Nielsen, H. Bildsoe, and H. J. Jakobsen, *J. Magn. Reson.* **95**, 88 (1991).
- ²⁵M. Baldus, B. H. Meier, R. R. Ernst, A. P. M. Kentgens, H. M. zu Altenschildesche, and R. Nesper, *J. Am. Chem. Soc.* **117**, 5141 (1995).
- ²⁶A. J. Vega, *J. Magn. Reson.* **96**, 50 (1992).
- ²⁷A. J. Vega, *Solid State Nucl. Magn. Reson.* **1**, 17 (1992).
- ²⁸G. Jeschke, *J. Chem. Phys.* **108**, 907 (1998).
- ²⁹D. Rovnyak, M. Baldus, and R. G. Griffin, *J. Magn. Reson.* **142**, 145 (2000).
- ³⁰G. Wu, D. Rovnyak, and R. G. Griffin, *J. Am. Chem. Soc.* **118**, 9326 (1996).
- ³¹D. Rovnyak, M. Baldus, and R. G. Griffin (unpublished).
- ³²S. A. Smith, T. O. Levante, B. H. Meier, and R. R. Ernst, *J. Magn. Reson.* **106**, 75 (1995).
- ³³See e.g., (a) J. H. Shirley, *Phys. Rev. B* **138**, 979 (1965); (b) A. Schmidt and S. Vega, *J. Chem. Phys.* **87**, 6895 (1987); (c) T. O. Levante, M. Baldus, B. H. Meier, and R. R. Ernst, *Mol. Phys.* **86**, 1195 (1995).
- ³⁴M. Baldus, T. O. Levante, and B. H. Meier, *Z. Naturforsch., A: Phys. Sci.* **49**, 80 (1994).
- ³⁵W. Sun, J. T. Stephen, L. D. Potter, and Y. Wu, *J. Magn. Reson., Ser. A* **116**, 181 (1995).
- ³⁶K. Takegoshi, K. Nomura, and T. Terao, *J. Magn. Reson.* **127**, 206 (1997).
- ³⁷(a) M. Baldus, M. Tomaselli, B. H. Meier, and R. R. Ernst, *Chem. Phys. Lett.* **230**, 329 (1994); (b) B. Q. Sun, P. R. Costa, D. Kocisko, P. T. Lansbury, and R. G. Griffin, *J. Chem. Phys.* **102**, 702 (1995).
- ³⁸See e.g., S. Hediger, B. H. Meier, N. D. Kurur, G. Bodenhausen, and R. R. Ernst, *Chem. Phys. Lett.* **223**, 283 (1994).
- ³⁹D. J. States, R. A. Haberkorn, and D. J. Ruben, *J. Magn. Reson.* **48**, 286 (1982).
- ⁴⁰P. Robyr, Ph.D. thesis, ETH Zurich, 1994, and reference therein; (b) M. Tomaselli, Ph.D. thesis, ETH Zurich, 1995, and references therein.
- ⁴¹B. H. Meier, *Adv. Magn. Opt. Reson.* **18**, 1 (1994).
- ⁴²K. Schmidt-Rohr and H. W. Spiess, *Multidimensional Solid-State NMR and Polymers* (Academic, New York, 1994).
- ⁴³S. P. Brown and S. Wimperis, *J. Magn. Reson.* **128**, 42 (1997).
- ⁴⁴See e.g., R. G. Griffin, *Nat. Struct. Biol.* **5**, 508 (1998), and references therein.
- ⁴⁵See e.g., J. Cavanagh, W. J. Fairbrother, A. G. Palmer III, and N. J. Skleton, *Protein NMR Spectroscopy: Principles and Practice* (Academic, San Diego, 1996).
- ⁴⁶G. S. Harbison, J. E. Roberts, J. Herzfeld, and R. G. Griffin, *J. Am. Chem. Soc.* **110**, 7221 (1988).
- ⁴⁷K. K. Kumashiro, K. Schmidt-Rohr, O. J. Murphy III, K. L. Ouellette, W. A. Cramer, and L. K. Thompson, *J. Am. Chem. Soc.* **120**, 5043 (1998).
- ⁴⁸C. A. Fyfe, J. Skibsted, H. Grondy, and H. M. Z. Altenschildesche, *Chem. Phys. Lett.* **281**, 44 (1998).